Chromatic Dispersion Manipulation Based on Optical Metasurfaces

Boyan Fu[1,3], Xiujuan Zou[1,3], Tao Li[1,2,3], Shuming Wang[1,2,3]*, Zhenlin Wang[1,3] and Shining Zhu[1,2,3]*

[1]*National Laboratory of Solid State Microstructures, School of Physics, College of Engineering and Applied Sciences, Nanjing University, Nanjing 210093, China*

[2]*Key Laboratory of Intelligent Optical Sensing and Manipulation Ministry of Education, Nanjing 210093, China*

[3]*Collaborative Innovation Center of Advanced Microstructures, Nanjing University, Nanjing 210093, China*

E-mail: wangshuming@nju.edu.cn, zhusn@nju.edu.cn

Abstract: Metasurfaces are densely arrayed two-dimensional (2D) artificial planar metamaterials, which can manipulate the polarization, distribution, and amplitude of light by accurately controlling the phase of the scattering light. The flat metasurface has the potential to substantially reduce the thickness and complexity of the structures and allows ease of fabrication and integration into devices. However, the inherent chromatic aberration of the metasurface originating from the resonant dispersion of the antennas and the intrinsic chromatic dispersion limit their quality. How to effectively suppress or manipulate the chromatic aberration of metalenses have attracted worldwide attention in the last few years, leading to a variety of excellent achievements. Furthermore, utilizing the chromatic dispersion of metasurface to realize special functionalities is also of significant importance. In this review, the most promising recent examples of chromatic dispersion manipulation based on optical metasurface materials are highlighted and put into perspective.

Keywords：metasurfaces; chromatic dispersion manipulation; achromatic metalenses

CLC number：O435.1；O436.3；O439

Sponsored by the

National Program on Key Basic Research Project of China (2017YFA0303700), National Natural Sci ence Foundation of China (No. 11621091, 11822406, 11774164, 11834007, 11774162).

1 Introduction

Over the past two decades, metamaterial, an artificial nanostructure based on subwavelength electromagnetic resonators (also known as meta-atom), have presented diverse and exotic properties[1-7]. Based on the revolutionary idea, plenty of achievements have been obtained, such as negative refractive index material[8], nonlinear harmonic generation[9-11], metalenses imaging[12, 13], optical cloaking[14], and even artificial black hole[15].

With the tailored permittivity and permeability distributions, metamaterials are able to control the propagation of light. However, they still utilize the propagation effect to manipulate the electromagnetic waves, which requires a complicated bulky structure. Fabrication of this three-dimensional (3D) metamaterials is a formidable challenge, especially in light frequency. Moreover, the loss cannot be ignored in such 3D structures, which greatly hinders the application of metamaterials.

In the past decade, metasurfaces, a two-dimensional (2D) or surface counterparts of metamaterials, have been proposed to overcome the above-mentioned problems[16]. The 2D nature of metasurfaces offers the possibility of lower loss, and the single layer configuration leads to easier fabrication process. Utilizing the resonances of the nanoantennas in the flat surface, metasurface can arbitrarily manipulate the parameters of light field, such as phase, amplitude, polarization, etc.[17-21]

In 2011, Capasso's group[16] introduced a generalized Snell's law of reflection and refraction to describe the propagation of light at the interface between two media with a phase discontinuity. By carefully designing the geometry of the V-shaped nanoantennas, the desired phase changes from 0 to 2π have been obtained, which is considered as the resonant phase metasurface (Fig. 1a). Based on this effective way for phase manipulation, many functions have been achieved, such as focusing or redirecting light[22, 23], controlling and modulating the state of polarization[24, 25] and tunable optical component[26-28]. However, it should be noted that resonant phase, which comes from electromagnetic (EM) resonance, relies on special incident wavelength and is required to control the phase profile with precise design and fabrication of the nanoantennas, limiting the development and extensive application. The geometric phase, also called Pancharatnam-Berry phase, is another way to manipulate phase change, which stems from circular polarization change[29] (Fig. 1b). Generally, EM waves generate an additional phase exp(i2α) during the conversion of the incident circularly polarized (CP) light to its opposite helicity with a rotating angle α of the antennas[30, 31] (Fig. 1c). The result is harnessed to acquire metasurfaces sensitive to circular polarized incident light. To make it easily understood, Poincaré sphere has also been shown in Fig. 1c. To be specific, if two parts of a uniformly polarized wave front are transported to a common polarization state along two different paths on the Poincaré sphere (polarization state space), the relative phase of the two light wave is half the corresponding solid angle of the closed path[32]. With the above-mentioned two principles, more light-manipulation properties and various conventional devices have been demonstrated, including control of phase and polarization[33-36], generation of novel holograms and holography[37-44], production of compact optical vortex beams[45-49], and even manipulation of light beam via digital coding metasurfaces[50, 51].

Despite of the powerful function in beam manipulation, an outstanding problem of optical elements based on metasurface lies in their strong chromatic aberrations which originates from the resonant meta-elements and diffractive nature of flat optical device. The dispersion of the

metasurface can be fine-tuned by manipulating the restriction of light within subwavelength nanoantennas, which is a more efficient method than that of refractive and Fresnel optics. For imaging applications, metasurface can exhibit sophisticated image corrections as well as eliminating the chromatic aberration over a continuous wavelength region. For some other devices, such as spectrometer, full-color router and nano-optic endoscope, chromatic dispersion manipulation by precise design in metasurfaces is also of great importance. Here the rapidly developing field of chromatic dispersion manipulation based on metasurface materials is highlighted, such as the achromatic metalens imaging and other special applications. First, the physical principles of achromatic aberration is summarized. Then the process of achromatic devices are described, especially the imaging and demonstrations of multiwavelength and continuous broadband achromatic lenses. Finally, some new exciting applications and research directions are outlined.

2 Principles of Chromatic Dispersion

Conventional optics suffers from chromatic aberrations on account of the accumulated phase dispersion during the light propagation. For normal dispersion, the refractive index decreases with increasing wavelength, thus the refractive optics in red light has smaller deflection angle and larger focal lengths than blue one. However, for the diffractive optical elements transmitted by means of amplitude or phase mask, the deflection angle increase with the increasing wavelength and the focal distance exhibit a negative correlation with the wavelength. This effect shows an opposite dispersion compared with normal refractive elements[52]. Thus, taking advantage of the opposite characteristics of the above two phenomena, integrating or cascading two or three optical elements was proposed to obtain ideal refractive or diffractive achromatic lenses. Although successful, these strategies add weight, cost and complexity in fabrication, and lose the metasurface superiority of unicity[53]. In addition, to obtain high spectral resolution, conventional spectrometer need a relatively long propagation distance to fully separate different wavelengths, leading to bulky and complex to fabricate.

The typical distribution of phase retardation for a focal lens is as follows[54]:

$$\varphi(R,\lambda) = -\left[2\pi\left(\sqrt{R^2+f^2}-f\right)\right]\frac{1}{\lambda} \qquad (1)$$

where $R = \sqrt{{x_0}^2 + {y_0}^2}$ is the distance from arbitrary position (x_0, y_0) on the lens to the center, and f is the focal length. Obviously, the required phase profile relies on the wavelength, resulting in the difficulty in precisely controlling phase at each desired wavelength at every position in order to achieve dispersion manipulation of metalens, such as achromatic focusing, super chromatic dispersion, reverse super chromatic dispersion, etc. For full-color optical applications, the performance in imaging and displaying is significantly affected by the dependence of the position or focal length on wavelength, thus a new method to achieve effective dispersion manipulation is required.

3 Manipulation of Chromatic Dispersion

3.1 Multiwavelength Achromatic Metasurfaces

In recent years, much effort has been focused on multiwavelength achromatic metadevices

for eliminating the chromatic dispersion and improving the performance of metalenses at a discrete set of wavelengths. To obtain equal focal distances at discrete wavelengths, the wavelength-dependent phase contribution needs to be provided to enable dispersive accumulated phase compensation in achromatic metasurface. Here the multi-wavelength achromatism in the infrared and visible wavelengths range is reviewed.

In 2015, Capasso group first proposed a metalens based on low-loss dielectric resonators[52], which introduces a dense spectrum of optical modes to compensate for dispersive phase at three infrared wavelengths of 1300 nm, 1550 nm, and 1800 nm with measured efficiencies of 9.8%, 10.3%, and 12.6% (Fig. 2a). In the later research, they designed and optimized the aperiodic array of the coupled dielectric resonators to generate different phase profile for each wavelength, experimentally demonstrating the new three efficiencies of 15%, 10%, and 21% at the same three wavelengths, as shown in Fig. 2b[55]. By utilizing the strong wavelength-dependent resonant phase in the coupled waveguide structures, a wavelength independent achromatic metalens is realized, which establishes an important first step towards the realization of achromatic optical metadevice. Besides, Faraon group also presented a method for designing double wavelength metasurfaces with two sets of unit elements. By suing the circular amorphous silicon nano-pillars, the polarization-insensitive and high-contrast transmission metalens, with a higher numerical aperture (NA) of 0.46, is realized (Fig. 2c). The metalens has the same focal length at 1550 nm and 915 nm, with the efficiencies of 65% and 22%, respectively[56]. In their later research, based on two spatially multiplexing methods, large scale segmentation and meta-atom interleaving have been employed to design two wavelength achromatic metalens with the same parameters as above. It should be noted that these methods enable the metalens to present additional working wavelength or functionalities (Fig. 2d)[57]. Besides, based on polarization dependent of two elliptical orthogonal polarizations independently, they proposed and demonstrated a double-wavelength metasurface that focuses light between 915 nm and 780 nm to the same focal length[58]. They experimentally demonstrated metasurface with high numerical apertures (up to 0.7) and high efficiencies($\eta \sim$ 65%-92%) at both wavelengths with nearly diffraction-limited operation, independently controlling the wavefronts at two different wavelengths for perpendicular polarizations. In addition, the two operating wavelengths can be set to any distance which is attractive for fluorescence microscopy applications. The unit elements, focusing effect, measured FWHMs, efficiencies, and axial or focal plane intensities are shown in Fig. 2e.

In 2016, Capasso group has successfully developed high-aspect-ratio metalens (with thickness of one hundred nanometers) based on TiO_2 nanoscale column unit in visible light range, and its single wavelength imaging performance can be comparable to the conventional optical microscope lens[18] (Fig. 3a). However, the chromatic aberration caused by material dispersion and diffraction effect is still an important challenge. Based on the development of the multiwavelength achromatic metalenses at infrared light, achromatism in visible light has gradually become the target of people's pursuit for their wider applications. Different from traditional optical lenses, cascaded or spatially diversified composite metal lenses are designed to meet the required phase distribution at a specific working wavelength. In order to reduce the chromatic aberrations of each diffractive component, Avayu et al.[59] demostrated dense triple vertically cascading of individual metasurfaces, where the layers are made from gold (Au) for red light, silver (Ag) for green light, and aluminium (Al) for blue light at wavelengths of 650 nm,

550nm, and 450 nm. The schematic diagrams of the triplet lens, the stacked nanodiscs, aberration correction for RGB light, the focal distance comparison of conventional Fresnel zone plate lens, and multilayered achromatic metalens are respectively shown in the left, middle, and right column of Fig. 3b, which confirms the ability of chromatic aberration correction of this method. This cascaded design is the first metasurface triplet lens of chromatic correction with various functionalities for red, green, and blue colors, addressing specific multifunctional optical requirements, which is quite similar with the traditional achromatism approach by using different dispersive optical materials. In addition, Lin et al.[60] eliminated the chromatic aberration of three primary colors (480 nm for blue, 550 nm for green, and 620 nm for red) by interleaved multiple distinct optical elements based on Si gradient metasurface(Fig. 3c). The three metalenses were separately designed to focus light at the same length and were randomly divided into some small segments which scattered among the entire area of the spatial metasurfaces. This method makes an important step towards multifunctional optical component patterned within a single surface area. Unlike the above multiwavelength metalenses combining several metalenses designed for particular frequencies into one, single metalens case based on appropriate meta-atoms design can also provide desired phase at different wavelengths.The birefringent dichroic meta-atom technique was used to experimentally confirm two-photon microscopy with a dual-wavelength metalens, which was specially designed to focus light at 820 nm and 605 nm to the same focal distance (Fig. 3d). Nevertheless, due to the interleaving and crosstalk between diverse structures designed for different wavelengths, the generated disturbing images and undesired diffraction levels will cause imaging quality degradation. The spatial multiplexing limits the maximum efficiency and complicated fabrication techniques are required in vertical stacking. In addition, the measured two-photon images was comparable to conventional objective lens in terms of quality and the focusing efficiency was 61% and 27% at 822 nm and 600 nm[61]. Similarly, Eisenbach et al.[62] demonstrated experimentally and by simulations the thin diffractive Fresnel zone plate metalenses with closely packed cross- and rod-shaped optical nano elements that focus two orthogonal polarizations at the wavelength of 460 nm and 650 nm to the same focal point (Fig. 3e).

Though the two methods mentioned above are powerful and effective for achromatic aberration with discrete wavelength, the dichroic birefringent principle and cross- and rod-shaped resonators limit working wavelengths range and require strong polarizations and wavelength selectivity. Another effective method to multiwavelength chromatic correction is the evolutionary optimized approach. Odom group introduced an achromatic metalenses based on evolutionary algorithm to achieve required optical responses by circularly rearranging the configuration of the nanoparticles on lattice. They utilized the lattice evolutionary algorithm combined with finite difference time domain method (FDTD) to simulate the optical fields and produce achromatic lattice lenses at 600 nm, 785 nm, and 980 nm through tuning various nanoparticle shapes[63] (Fig. 3f). It can be anticipated that the design method could extend to wider range of wavelengths. Different from the previous methods of spatial multiplexing and vertical stack, Capasso group reported a versatile metasurface with flexible dispersion and diverse function and designed a multiwavelength achromatic metalens for four wavelengths in the visible spectrum through a wavelength independent phase profile encoded in a phase shifter. Besides, they also designed two wavelength-dependent beam generators. One focuses beams with different orbital angular momentum states at red, green, and blue, respectively, and the

other is focused for red and green light, while generating a vortex beam for blue[64] (Fig. 3g). For comparison, the specific parameters of the lens have been listed in Table 1.

3.2 Continuously Achromatic Metasurfaces

With the increase of the bandwidth required for more applications, the desire for new methods or mechanisms to realize the continuous achromatic correction is more intense. At present, the mainly challenge is to design achromatic metalens that generates a single focal spot over a wide wavelength range. The difficulty lies in simultaneously engineering phase profiles at any wavelengths produced from a single metasurface. In recent years, new ideas have been put forward to achieve broadband continuous achromatism. This review still divides it into infrared light and visible light to discuss the methods or mechanisms separately.

Faraon and co-workers took advantage of reflective metasurface based on dielectric nanoantennas to demonstrate achromatic dispersion-controlled metalenses with positive, zero, and hyper-dispersion operating over a narrowband in infrared. The nano-posts covering phase of 0-2$\pi$and providing different phase dispersions and the measured focusing efficiency at different wavelengths shows in Fig. 4a, respectively. Besides, the measured result shows a highly reduced chromatic dispersion with general efficiency between 50% and 60% over the whole wavelength range of 1490-1550 nm and shows no significant reduction compared to the regular metalens[65]. But for every specific functional meatasurface, a great deal of calculations is required to satisfy its unique phase compensation. New design idea of achromatic metalens over a broad wavelength range is still required.

Wang et al.[54] constructed a revolutionary design method of combining the resonant phase and the geometric phase to eliminate the chromatic aberration of circular polarization incidence in the continuous wavelength range of 1200 nm to 1680 nm in a reflection scheme. Generally, for the case of working wavelength band (λ_{min}, λ_{max}), the phase in Eq. (1) can be split into

$$\varphi(\mathrm{R},\lambda) = \varphi(\mathrm{R},\lambda_{max}) + \Delta\varphi(\mathrm{R},\lambda) \qquad (2)$$

By using geometric phase as the phase modulation of each metalense, the former wavelength independent phase profile in Eq. (2) can be obtained. In contrast, the latter one is the phase difference of variable incident wavelengths and follows a linear relation with $1/\lambda$, which can be required by appropriately designing the phase response of each element on metalens. Then, combining Eq. (1) and (2), the phase profile of achromatic metal could be rewritten as

$$\varphi'_{Lens}(R,\lambda) = -\left[2\pi\left(\sqrt{R^2+f^2}-f\right)\right]\frac{1}{\lambda} + \varphi_{shift} \qquad (3)$$

The additional φ_{shift} is to realize the desired phase compensation profile from specially designed blocks at each sampling positions. The basic building block design, the SEM of fabricated metalenses, the measured and simulated focal length, and intensity profiles of different incident wavelengths are exhibited in Fig. 4b. However, the design principle requires metalenses working at circularly polarized incidence, limiting some other applications. In later research, Shrestha et al.[66] demonstrated a CMOS-compatible broadband achromatic metalens for arbitrary polarizated incident light waves from 1200 nm to 1650 nm in the near infrared wavelengths. They created libraries of meta-units to design metasurfaces with varying geometrical parameters to satisfy various phase profile and derived the limitations of achromatic metalens performance. Then, they experimentally demonstrated the efficiencies of some polarization-independent

achromatic metalenses is up to 50%, as shown in Fig. 4c.

Generally, though the achromatic metalens designed for infrared regime are useful in several applications, optical metadevices are highly desirable and much more attractive in the visible spectrum. Following the previous principle, Wang et al.[67] further designed and fabricated a GaN-based broadband achromatic metalens composed of various size of subwavelength periodic hexagonal pillars and inverse one at the range of 400 nm to 660 nm in transmission mode. As a high refractive semiconductor material, GaN is an ideal choice to be intergrated resonant unit elements due to high hardness, stability, and low loss. Besides, With exciting higher orders of waveguide-like resonant modes, GaN nanopillars can obtain large phase compensation while increasing the height of the nanopillars. They therefore used inverse high-aspect ratio nanopillars of 800nm for a large phase compensation and successfully eliminate chromatic aberration at about 49% bandwidth of the central working wavelength(Fig. 5a). In addition, another further broadband achromatic gradient metasurface based on aluminum was similarly designed in the range of 400 nm to 667 nm with the efficiency of above 20%[68]. They experimently verified three achromatic deflectors eliminating chromatic aberration at about 50% bandwidth of the central working wavelength and applyed to construct a versatile polarization convertor which can simultaneously generate six polarization states(Fig. 5b).

By judicious design of TiO_2 nanofins on metasurface, which is different from spatial multiplexing or cascading, Capasso group demonstrated a new method to design the phase profile and simultaneously control the phase and group delay dispersion, thereby engineering a transmissive achromatic metalens over a wide continuous band in the visible spectrum(from 470 nm to 670 nm)[69]. In this work, Eq. (1) can be expressed as a Taylor expansion near a constant frequency ω_d as

$$\varphi(\mathrm{R},\omega) = \varphi(\mathrm{R},\omega_d) + \frac{\partial\varphi(\mathrm{R},\omega)}{\partial\omega}\Big|_{\omega=\omega_d}(\omega-\omega_d) + \frac{\partial^2\varphi(\mathrm{R},\omega)}{2\partial\omega^2}\Big|_{\omega=\omega_d}(\omega-\omega_d)^2 \quad (4)$$

Therefore, higher-order terms turned into an essential consideration for phase and group delay to realize the diffraction limited focusing over a broad wide wavelengths. Besides, it is a a significant advance that they digitized the phase and group delay and selected elements from the various nanofin parameters library to design desired achromatic metalenses. However, polarization-insensitive metasurfaces are much more attractive and highly desirable for many applications, and generally limit the chosen elements to isotropic nanostructures. In their later research, they designed a polarization-insensitive metacorrector with anisotropic nanofins to correct spherical and chromatic aberrations through combining a tunable phase and artificial dispersion[70]. As a proof of concept, the achromatism range of metacorrectors is nearly the entire visible and even extends significantly to the bandwidth of state-of-the-art immersion objective. Similarly, the phase, group delay and group delay dispersion related to frequency in Eq. (4) were implemented by correspondingly size of nanofins to realize the broadband achromatic metalens in both simulations and experiments. The hybrid lens consisting of a metacorrector, a spherical lens, phase profiles for varying incident wavelengths, SEM, and imaging effect can be seen in Fig. 5c. After that, they also demonstrated another polarization-insensitive metasurface with multiple anisotropic nanofins to additional degrees of freedom which can better control the dispersion and phase of the output light[71]. They also swept the parameters of the nanofits to build a library and fabricated a metalens with a numerical aperture (NA) of 0.2, exhibiting continuous focusing from 460 nm to 700 nm. The SEM of nanofins selection and design, focusing

effect and imaging effect are shown in Fig. 5d.

In addition, some other continuous achromatic metalenses researches were designed at mid-infrared and terahertz regime. Mid-infrared devices based on metalenses are of great utility in the fields of imaging, space communication, and molecule sensing. Zhou et al.[72] proposed an infrared circularly polarized achromatic metalens that can operate over the wavelengths from 3.7 μm to 4.5 μm through varying the size of the Si blocks (standing on a CaF2 substrate) to satisfy the required phase compensation between λ_{min} and λ_{max}. They utilized the same design mechanism of separating the geometric phase and resonant phaseto manipulate the wavefront and eliminate the chromatic aberration. The metalens element and measured intensity profiles of the focal spot are shown in Fig. 6a. Moreover, Cheng et al.[73] proposed a broadband achromatic metalens in terahertz regime from 0.3 to 0.8 THz. In order to acquire a more robust phase accumulation, they chose C-shaped unit elements to fabricate terahertz achromatic metalens(Fig. 6b). Terahertz achromatic metalenses can be utilized in many special applications, such as spectroscopy, time-off light tomography, and hyperspectral imaging systems, etc. For comparison, some specific parameters of the continuous achromatic metalenses have been listed in Table 2.

3.3 Superdispersive Elements

How to eliminate dispersion to obtain a clear image has been emphasized above, but sometimes in practical applications it is often needed to expand the dispersion. In other words, it is also necessary to modulate a large dispersion to achieve the function of separating electromagnetic waves of different wavelengths. Large dispersion is often pursued for some optical applications, such as wavelength division multiplexing and the spectroscopic analysis. Expansion of dispersion also requires the use of dispersion modulation of the wavefront, which often has the same principles as that of elimination of dispersion. Thus, many works demonstrated simultaneously an achromatic metalens and a superdispersive metalens with the same designing methodology. Li et al.[74] designed a series of flat dielectric metasurface lenses for three discrete wavelengths of 473 nm, 532 nm, and 632.8 nm attributed by unique dispersion engineering ability of metasurface. They utilized three distinct nanostructures to respectively dominate three wavelengths and then construct interleaved rotating nanostructure into the surface of metalens. Great effects of achromatic metalenses and several super-dispersion metalenses with different wavelengths focused on arbitrary special positions are achieved in simulation in Fig. 7a. Khorasaninejad et al.[75] proposed a method to achieve an achromatic metalens and a metalens with reverse chromatic dispersion over a continuous range of wavelengths from 490 nm to 550 nm. By optimizing each unit cells' geometric parameters to achieve phase coverage of 0-2π and utilizing the particle swarm optimization algorithm, the metalenses with tailored chromatic dispersion are demonstrated successfully, as shown in Fig. 7b.

Capasso's group designed and fabricated a superdispersive metalens with very fine wavelength resolution of 200 pm in the telecom range[76]. As shown in Fig. 7c, the metalens consisting of silicon nanofins is designed to acquire large angle, off-axis focusing, and high efficiencies reaching 90% in the infrared region from 1100 nm to 1600 nm. High spectral resolution is realized for a wider wavelength range by stitching several metalenses together. Thus, the high-efficiency metalens can be utilized for multispectral imaging due to its super-dispersive. Different from the principle of the above-mentioned research that superdispersive

metalens is obtained by enhancing the intrinsic dispersion, Faraon's group demonstrated a folded compact spectrometer with spectral resolution of about 1.2 nm in the near-infrared region[77]. Based on the traditional diffraction spectrometer, they proposed a scheme that has dispersive and focusing metasurfaces on the side of the transparent substrate. Different input wavelengths from 760 nm to 860 nm are designed to focus at different position along y-axis direction. They experimentally measured intensity distributions for two input wavelengths that are 1.25 nm apart for TE and TM polarizations, illustrating that the experimental spectral resolution is slightly worse than the simulated spectral resolution (of 1.1 nm) due to some practical imperfection (Fig. 7d). Additionally, the folded spectrometer can measure the spectrum of a wideband source and the optical depth of an Nd:YVO4 crystal sample, showing the results in good agreement with commercial spectrometers. For comparison, the state-of-the-art achievements on achromatic and super dispersion metalenses are summarized in Fig. 8.

3.4 Some Advanced Applications Based on Dispersion Manipulation

Apart from the above-mentioned proofs of concept, various applications of controlling chromatic dispersion with metasurfaces including light-field camera, full-color routing, nano-optic endoscope, and multiwavelength achromatic holograms will be discussed below.

Lin et al.[78] fabricated a GaN-based 60×60 achromatic metalens array to realize a full color light-field camera, which can capture spatial scene information and reconstruct the rendered images on the depth of field through measuring the intensity and the direction of incident light(left of Fig. 9a). More importantly, the relative speed data can be proved while assessing the depths and directions of multiple objects, and thus achieving the optical 4D information. They therefore rendered the patch optimization of diverse depths according to the 4D information and exhibited the refocused high resolution images(right of Fig. 9a). Generally, full-color achromatic light-field cameras could be utilized in the fields of self-driving vehicles, robotic vision, and virtual and augmented reality.

Chen et al.[79] firstly demonstrated three individual high efficiency metalenses based on GaN and then experimentally verified a multiplex color router with dielectric metalens, which can be designed to focus the red, green,and blue input light to arbitiary spatial positions(Fig. 9b). The full-color routing device is of high efficiency for the larger collection area of white light, reaching 87%, 91.6%, and 50.6% for blue, green, and red lights, respectively. The new method of color routing on GaN metalens is extraordinary applicable to integrated optical devices for the high efficiency, semiconductor compatibility and low cost. In addition, with high degree of freedom and flexible phase manipulation of input light at subwavelength level, Pahlevaninezhad et al.[80] put forward another clinical application of nano-optic endoscope with metasurfaces to acquire near diffraction-limited imaging. The polarization independent metalens composed of α-Si unit elements with various diameters to satisfy the phase profile with the output wavelengths from 1250 nm to 1370 nm.

Achromatic and super-dispersive hologram is another important application for dielectric metasurfaces. Wang et al.[81] exhibited silica-based achromatic and highly dispersive meta-holograms composed of three kinds of nanopillars with different orientations of rotation in visible regime. They changed the orientations of the corresponding nanoblocks to attain the full phase control and induce required geometric phases. The desired image containing three independent parts of red flower, green peduncle, and blue pot was rebuilt at three lasers of 633 nm, 532 nm, and 473 nm (Fig. 9c). However, if only one laser is used, each part will appear

separately at different locations, confirming three individual channels without cross-talk.This technique will find numerous applications with independent wavefront control over a broad range of wavelengths.

In addition, Chen et al.[82] applied large chromatic dispersion to tomographic imaging in order to realize spectral focus tuning in the visible spectrum. They first designed an aplanatic metalens with large chromatic dispersion and applied it to a spectral 3D tomographic imaging. Objects with different depths arranged along the optical axis are better imaged using the designed aplanatic metalens under different incident wavelengths without any moving elements than that of normal metalens, confirming the ability of the depth-of-field resolution. Additionally, using a kind of biocells (frog egg cells) as 3D object, researchers pictured a group of microscopic images from the metalens-based tomographic imaging setup as shown in Fig. 9d. These microscopic images with relatively realistic morphology and inner structures of the frog cells can be distinguished, demonstrating the effectiveness of the aplanatic metalens.

4 Conclusions and Discussion

Metasurface devices have presented their potential to complement, even replace, their traditional counterparts due to their flexibility of tailoring electromagnetic scattering. To sum up, the recent development of chromatic dispersion manipulation based on metasurfaces have been reviewed. Various approaches for chromatic aberration correction have been proposed to realize multiwavelength achromatism, continuous achromatism in infrared, visible, and even terahertz region, respectively. It is worth noting that the achromatic metalenses with relatively large NA and high efficiency in visible region has the potential for promising applications for commercial purposes,such as cell phone camera modules, virtual reality field, and machine vision. Moreover, the monochromatic dispersion can also be attractive in many special applications, such as spectrometer and multicolor hologram, etc. In addition, another interest on metasurface is focusing beams to one desire focal point regardless of the angle of incidence (termed angular phase control), which is applicable to bioimaging and endoscopy, etc. The sophisticated tasks on chromatic dispersion manipulation can fuel the continuous progress of portable electronics and optics with low-cost and high-performance miniaturized systems.

References

[1] Jahani SJacob Z. All-dielectric metamaterials. Nature Nanotechnology, 2016, 11(1): 23-36. DOI: 10.1038/nnano.2015.304.

[2] Kuznetsov A I, Miroshnichenko A E, Brongersma M L, et al. Optically resonant dielectric nanostructures. Science, 2016, 354(6314). DOI: 10.1126/science.aag2472.

[3] Nicholls L H, Rodríguez-Fortuño F J, Nasir M E, et al. Ultrafast synthesis and switching of light polarization in nonlinear anisotropic metamaterials. Nature Photonics, 2017, 11(10): 628-633. DOI: 10.1038/s41566-017-0002-6.

[4] Cheben P, Halir R, Schmid J H, et al. Subwavelength integrated photonics. Nature, 2018, 560(7720): 565-572. DOI: 10.1038/s41586-018-0421-7.

[5] Jahani S, Kim S, Atkinson J, et al. Controlling evanescent waves using silicon photonic all-dielectric metamaterials for dense integration. Nature Communications, 2018, 9(1): p.1893. DOI: 10.1038/s41467-018-04276-8.

[6] Lin J, Mueller J P B, Wang Q, et al. Polarization-Controlled Tunable Directional Coupling of Surface Plasmon Polaritons. Science, 2013, 340(6130): 331-334. DOI: 10.1126/science.1233746.

[7] Zhu A Y, Kuznetsov A I, Luk'yanchuk B, et al. Traditional and emerging materials for optical metasurfaces. Nanophotonics, 2017, 6(2): 452-471. DOI: 10.1515/nanoph-2016-0032.

[8] Huang L, Chen X, Mühlenbernd H, et al. Dispersionless Phase Discontinuities for Controlling Light Propagation. Nano Letters, 2012, 12(11): 5750-5755. DOI: 10.1021/nl303031j.

[9] Celebrano M, Wu X, Baselli M, et al. Mode matching in multiresonant plasmonic nanoantennas for enhanced second harmonic generation. Nature Nanotechnology, 2015, 10(5): 412-7. DOI: 10.1038/nnano.2015.69.

[10] Smirnova D A, Khanikaev A B, Smirnov L A, et al. Multipolar Third-Harmonic Generation Driven by Optically Induced Magnetic Resonances. Acs Photonics, 2016, 3(8): 1468-1476. DOI: 10.1021/acsphotonics.6b00036.

[11] Kauranen MZayats A V. Nonlinear plasmonics. Nature Photonics, 2012, 6(11): 737-748. DOI: 10.1038/nphoton.2012.244.

[12] Khorasaninejad M, Chen W T, Zhu A Y, et al. Multispectral Chiral Imaging with a Metalens. Nano Letters, 2016, 16(7): 4595-600. DOI: 10.1021/acs.nanolett.6b01897.

[13] Chen W T, Zhu A Y, Khorasaninejad M, et al. Immersion Meta-Lenses at Visible Wavelengths for Nanoscale Imaging. Nano Letters, 2017, 17(5): 3188-3194. DOI: 10.1021/acs.nanolett.7b00717.

[14] Ni X, Wong Z J, Mrejen M, et al. An ultrathin invisibility skin cloak for visible light. Science, 2015, 349(6254): 1310-1314. DOI: 10.1126/science.aac9411.

[15] Sheng C, Liu H, Wang Y, et al. Trapping light by mimicking gravitational lensing. Nature Photonics, 2013, 7(11): 902-906. DOI: 10.1038/nphoton.2013.247.

[16] Yu N, Genevet P, Kats M A, et al. Light propagation with phase discontinuities: generalized laws of reflection and refraction. Science, 2011, 334(6054): 333-7. DOI: 10.1126/science.1210713.

[17] Wang L, Kruk S, Tang H, et al. Grayscale transparent metasurface holograms. Optica, 2016, 3(12): 1504-1505. DOI: 10.1364/optica.3.001504.

[18] Khorasaninejad M, Chen W T, Devlin R C, et al. Metalenses at visible wavelengths: Diffraction-limited focusing and subwavelength resolution imaging. Science, 2016, 352(6290): 1190-1194. DOI: 10.1126/science.aaf6644.

[19] Zang W, Yuan Q, Chen R, et al. Chromatic Dispersion Manipulation Based on Metalenses. Advanced Materials, 2019: p.1904935. DOI: 10.1002/adma.201904935.

[20] Khorasaninejad MCapasso F. Metalenses: Versatile multifunctional photonic components. Science, 2017, 358(6367). DOI: 10.1126/science.aam8100.
[21] Zou X, Zheng G, Yuan Q, et al. Imaging based on metalenses. PhotoniX, 2020, 1(1): p.2. DOI: 10.1186/s43074-020-00007-9.
[22] Sun S, Yang K Y, Wang C M, et al. High-efficiency broadband anomalous reflection by gradient meta-surfaces. Nano Letters, 2012, 12(12): 6223-9. DOI: 10.1021/nl3032668.
[23] Fattal D, Li J, Peng Z, et al. Flat dielectric grating reflectors with focusing abilities. Nature Photonics, 2010, 4(7): 466-470. DOI: 10.1038/nphoton.2010.116.
[24] Chen H, Wang J, Ma H, et al. Ultra-wideband polarization conversion metasurfaces based on multiple plasmon resonances. Journal of Applied Physics, 2014, 115(15): p.154504. DOI: 10.1063/1.4869917.
[25] Chen W T, Torok P, Foreman M R, et al. Integrated plasmonic metasurfaces for spectropolarimetry. Nanotechnology, 2016, 27(22): p.224002. DOI: 10.1088/0957-4484/27/22/224002.
[26] Huang Y W, Lee H W, Sokhoyan R, et al. Gate-Tunable Conducting Oxide Metasurfaces. Nano Letters, 2016, 16(9): 5319-25. DOI: 10.1021/acs.nanolett.6b00555.
[27] Sherrott M C, Hon P W C, Fountaine K T, et al. Experimental Demonstration of >230 degrees Phase Modulation in Gate-Tunable Graphene-Gold Reconfigurable Mid-Infrared Metasurfaces. Nano Letters, 2017, 17(5): 3027-3034. DOI: 10.1021/acs.nanolett.7b00359.
[28] Wu P C, Papasimakis NTsai D P. Self-Affine Graphene Metasurfaces for Tunable Broadband Absorption. Physical Review Applied, 2016, 6(4): p.044019. DOI: 10.1103/PhysRevApplied.6.044019.
[29] Berry M V. QUANTAL PHASE-FACTORS ACCOMPANYING ADIABATIC CHANGES. Proceedings of the Royal Society of London Series a-Mathematical and Physical Sciences, 1984, 392(1802): 45-57. DOI: 10.1098/rspa.1984.0023.
[30] Pancharatnam S. Generalized theory of interference and its applications. Proceedings of the Indian Academy of Sciences - Section A, 1956, 44(6): 398-417. DOI: 10.1007/BF03046095.
[31] Chen X, Huang L, Muhlenbernd H, et al. Dual-polarity plasmonic metalens for visible light. Nature Communications, 2012, 3: p.1198. DOI: 10.1038/ncomms2207.
[32] Hu Z, Xu T, Tang R, et al. Geometric-phase metasurfaces: from physics to applications. Laser & Optoelectronics Progress, 2019, 56(20): 113-133. DOI: 10.3788/lop56.202403.(in Chinese)
[33] Arbabi A, Horie Y, Bagheri M, et al. Dielectric metasurfaces for complete control of phase and polarization with subwavelength spatial resolution and high transmission. Nature Nanotechnology, 2015, 10(11): 937-43. DOI: 10.1038/nnano.2015.186.
[34] Balthasar Mueller J P, Rubin N A, Devlin R C, et al. Metasurface Polarization Optics: Independent Phase Control of Arbitrary Orthogonal States of Polarization. Physical Review Letters, 2017, 118(11). DOI: 10.1103/PhysRevLett.118.113901.
[35] Wu P C, Tsai W Y, Chen W T, et al. Versatile Polarization Generation with an Aluminum Plasmonic Metasurface. Nano Letters, 2017, 17(1): 445-452. DOI: 10.1021/acs.nanolett.6b04446.
[36] Chen W T, Yang K Y, Wang C M, et al. High-efficiency broadband meta-hologram with polarization-controlled dual images. Nano Letters, 2014, 14(1): 225-30. DOI: 10.1021/nl403811d.
[37] Ni X, Kildishev A VShalaev V M. Metasurface holograms for visible light. Nature Communications, 2013, 4(1): p.2807. DOI: 10.1038/ncomms3807.
[38] Zheng G, Muhlenbernd H, Kenney M, et al. Metasurface holograms reaching 80% efficiency. Nature Nanotechnology, 2015, 10(4): 308-12. DOI: 10.1038/nnano.2015.2.

[39] Huang K, Dong Z, Mei S, et al. Silicon multi-meta-holograms for the broadband visible light. Laser & Photonics Reviews, 2016, 10(3): 500-509. DOI: 10.1002/lpor.201500314.
[40] Khorasaninejad M, Ambrosio A, Kanhaiya P, et al. Broadband and chiral binary dielectric meta-holograms. Science Advances, 2016, 2(5). DOI: 10.1126/sciadv.1501258.
[41] Li X, Chen L, Li Y, et al. Multicolor 3D meta-holography by broadband plasmonic modulation. Science Advances, 2016, 2(11). DOI: 10.1126/sciadv.1601102.
[42] Wen D, Yue F, Li G, et al. Helicity multiplexed broadband metasurface holograms. Nature Communications, 2015, 6: p.8241. DOI: 10.1038/ncomms9241.
[43] Huang L, Chen X, Mühlenbernd H, et al. Three-dimensional optical holography using a plasmonic metasurface. Nature Communications, 2013, 4(1): p.2808. DOI: 10.1038/ncomms3808.
[44] Huang Y W, Chen W T, Tsai W Y, et al. Aluminum plasmonic multicolor meta-hologram. Nano Letters, 2015, 15(5): 3122-7. DOI: 10.1021/acs.nanolett.5b00184.
[45] Yang Y, Wang W, Moitra P, et al. Dielectric Meta-Reflectarray for Broadband Linear Polarization Conversion and Optical Vortex Generation. Nano Letters, 2014, 14(3): 1394-1399. DOI: 10.1021/nl4044482.
[46] Li G, Kang M, Chen S, et al. Spin-Enabled Plasmonic Metasurfaces for Manipulating Orbital Angular Momentum of Light. Nano Letters, 2013, 13(9): 4148-4151. DOI: 10.1021/nl401734r.
[47] Yue F, Wen D, Xin J, et al. Vector Vortex Beam Generation with a Single Plasmonic Metasurface. Acs Photonics, 2016, 3(9): 1558-1563. DOI: 10.1021/acsphotonics.6b00392.
[48] Genevet P, Yu N, Aieta F, et al. Ultra-thin plasmonic optical vortex plate based on phase discontinuities. Applied Physics Letters, 2012, 100(1): p.013101. DOI: 10.1063/1.3673334.
[49] Shen Y, Wang X, Xie Z, et al. Optical vortices 30 years on: OAM manipulation from topological charge to multiple singularities. Light: Science & Applications, 2019, 8: p.90. DOI: 10.1038/s41377-019-0194-2.
[50] Cui T J, Liu S, Bai G D, et al. Direct Transmission of Digital Message via Programmable Coding Metasurface. Research (Washington, D.C.), 2019, 2019: 2584509-2584509. DOI: 10.34133/2019/2584509.
[51] Zhang L, Chen X Q, Liu S, et al. Space-time-coding digital metasurfaces. Nature Communications, 2018, 9(1): p.4334. DOI: 10.1038/s41467-018-06802-0.
[52] Aieta F, Kats M A, Genevet P, et al. Multiwavelength achromatic metasurfaces by dispersive phase compensation. Science, 2015, 347(6228): 1342-1345. DOI: 10.1126/science.aaa2494.
[53] Tseng M L, Hsiao H-H, Chu C H, et al. Metalenses: Advances and Applications. Advanced Optical Materials, 2018, 6(18): p.1800554. DOI: 10.1002/adom.201800554.
[54] Wang S, Wu P C, Su V C, et al. Broadband achromatic optical metasurface devices. Nature Communications, 2017, 8(1): p.187. DOI: 10.1038/s41467-017-00166-7.
[55] Khorasaninejad M, Aieta F, Kanhaiya P, et al. Achromatic Metasurface Lens at Telecommunication Wavelengths. Nano Letters, 2015, 15(8): 5358-62. DOI: 10.1021/acs.nanolett.5b01727.
[56] Arbabi E, Arbabi A, Kamali S M, et al. Multiwavelength polarization-insensitive lenses based on dielectric metasurfaces with meta-molecules. Optica, 2016, 3(6): 628-633. DOI: 10.1364/optica.3.000628.
[57] Arbabi E, Arbabi A, Kamali S M, et al. Multiwavelength metasurfaces through spatial multiplexing. Scientific Reports, 2016, 6: p.32803. DOI: 10.1038/srep32803.
[58] Arbabi E, Arbabi A, Kamali S M, et al. High efficiency double-wavelength dielectric metasurface

lenses with dichroic birefringent meta-atoms. Optics Express, 2016, 24(16): 18468-77. DOI: 10.1364/OE.24.018468.
[59] Avayu O, Almeida E, Prior Y, et al. Composite functional metasurfaces for multispectral achromatic optics. Nature Communications, 2017, 8: p.14992. DOI: 10.1038/ncomms14992.
[60] Lin D, Holsteen A L, Maguid E, et al. Photonic Multitasking Interleaved Si Nanoantenna Phased Array. Nano Letters, 2016, 16(12): 7671-7676. DOI: 10.1021/acs.nanolett.6b03505.
[61] Arbabi E, Li J, Hutchins R J, et al. Two-Photon Microscopy with a Double-Wavelength Metasurface Objective Lens. Nano Letters, 2018, 18(8): 4943-4948. DOI: 10.1021/acs.nanolett.8b01737.
[62] Eisenbach O, Avayu O, Ditcovski R, et al. Metasurfaces based dual wavelength diffractive lenses. Optics Express, 2015, 23(4): 3928-36. DOI: 10.1364/OE.23.003928.
[63] Hu J, Liu C H, Ren X, et al. Plasmonic Lattice Lenses for Multiwavelength Achromatic Focusing. ACS Nano, 2016, 10(11): 10275-10282. DOI: 10.1021/acsnano.6b05855.
[64] Shi Z, Khorasaninejad M, Huang Y W, et al. Single-Layer Metasurface with Controllable Multiwavelength Functions. Nano Letters, 2018, 18(4): 2420-2427. DOI: 10.1021/acs.nanolett.7b05458.
[65] Arbabi E, Arbabi A, Kamali S M, et al. Controlling the sign of chromatic dispersion in diffractive optics with dielectric metasurfaces. Optica, 2017, 4(6): 625-632. DOI: 10.1364/optica.4.000625.
[66] Shrestha S, Overvig A C, Lu M, et al. Broadband achromatic dielectric metalenses. Journal, 2018,7(Issue): 85. 10.1038/s41377-018-0078-x.
[67] Wang S, Wu P C, Su V-C, et al. A broadband achromatic metalens in the visible. Nature Nanotechnology, 2018, 13(3): 227-232. DOI: 10.1038/s41565-017-0052-4.
[68] Hsiao H-H, Chen Y H, Lin R J, et al. Integrated Resonant Unit of Metasurfaces for Broadband Efficiency and Phase Manipulation. Advanced Optical Materials, 2018, 6(12): p.1800031. DOI: 10.1002/adom.201800031.
[69] Chen W T, Zhu A Y, Sanjeev V, et al. A broadband achromatic metalens for focusing and imaging in the visible. Nature Nanotechnology, 2018, 13(3): 220-226. DOI: 10.1038/s41565-017-0034-6.
[70] Chen W T, Zhu A Y, Sisler J, et al. Broadband Achromatic Metasurface-Refractive Optics. Nano Letters, 2018, 18(12): 7801-7808. DOI: 10.1021/acs.nanolett.8b03567.
[71] Chen W T, Zhu A Y, Sisler J, et al. A broadband achromatic polarization-insensitive metalens consisting of anisotropic nanostructures. Nature Communications, 2019, 10(1): p.355. DOI: 10.1038/s41467-019-08305-y.
[72] Zhou H, Chen L, Shen F, et al. Broadband Achromatic Metalens in the Midinfrared Range. Physical Review Applied, 2019, 11(2): p.024066. DOI: 10.1103/PhysRevApplied.11.024066.
[73] Cheng Q, Ma M, Yu D, et al. Broadband achromatic metalens in terahertz regime. Science Bulletin, 2019, 64(20): 1525-1531. DOI: 10.1016/j.scib.2019.08.004.
[74] Li K, Guo Y, Pu M, et al. Dispersion controlling meta-lens at visible frequency. Optics Express, 2017, 25(18): 21419-21427. DOI: 10.1364/OE.25.021419.
[75] Khorasaninejad M, Shi Z, Zhu A Y, et al. Achromatic Metalens over 60 nm Bandwidth in the Visible and Metalens with Reverse Chromatic Dispersion. Nano Letters, 2017, 17(3): 1819-1824. DOI: 10.1021/acs.nanolett.6b05137.
[76] Khorasaninejad M, Chen W T, Oh J, et al. Super-Dispersive Off-Axis Meta-Lenses for Compact High Resolution Spectroscopy. Nano Letters, 2016, 16(6): 3732-7. DOI: 10.1021/acs.nanolett.6b01097.
[77] Faraji-Dana M, Arbabi E, Arbabi A, et al. Compact folded metasurface spectrometer. Nature Communications, 2018, 9(1): p.4196. DOI: 10.1038/s41467-018-06495-5.

[78] Lin R J, Su V C, Wang S, et al. Achromatic metalens array for full-colour light-field imaging. Nature Nanotechnology, 2019, 14(3): 227-231. DOI: 10.1038/s41565-018-0347-0.
[79] Chen B H, Wu P C, Su V C, et al. GaN Metalens for Pixel-Level Full-Color Routing at Visible Light. Nano Letters, 2017, 17(10): 6345-6352. DOI: 10.1021/acs.nanolett.7b03135.
[80] Pahlevaninezhad H, Khorasaninejad M, Huang Y W, et al. Nano-optic endoscope for high-resolution optical coherence tomography in vivo. Nature Photonics, 2018, 12(9): 540-547. DOI: 10.1038/s41566-018-0224-2.
[81] Wang B, Dong F, Li Q T, et al. Visible-Frequency Dielectric Metasurfaces for Multiwavelength Achromatic and Highly Dispersive Holograms. Nano Letters, 2016, 16(8): 5235-40. DOI: 10.1021/acs.nanolett.6b02326.
[82] Chen C, Song W, Chen J W, et al. Spectral tomographic imaging with aplanatic metalens. Light: Science & Applications, 2019, 8: p.99. DOI: 10.1038/s41377-019-0208-0.

Table 1 Optical parameters of multiwavelength achromatic metalenses

Reference	Wavelength (nm)	Efficiency (%)	FWHM (um)	Numerical aperture (NA)	Diameter (um)	Focal distance(mm)	Material	Polarization
[52]	1300 1550 1800	9.8 10.3 12.6	~ 0.03	0.05	600	7.5	Si/SiO_2	Insensitive
[55]	1300 1550 1800	15 10 21	27.5 29 25	0.04	600	7.5	Si/SiO_2	Insensitive
[56]	1550 915	65 22	2.9 1.9	0.46	300	0.286	Si/SiO_2	Insensitive
[57]	1550	30 58	3.3	0.46	300	0.4	Si/SiO_2	Insensitive
	915	37 10	1.85					
[58]	915 780	65~92	1~4	0.12~0.7	200	0.1/0.2/0.4/0.6/0.8	Si/SiO_2	Linear (cross)
[18]	405 532 660	86 73 66	280 375 450	0.8	240	0.09	TiO_2/SiO_2	Circle (cross)
[59]	650 550 450	5.8-8.7	2.6 2. 43 2.11	---	0.125 0.085 0.12	1	Au Ag Al/SiO_2	Insensitive
[60]	620 550 480	---	~0.683	0.43	96	100	Si/glass	Circle
[61]	605 820	27 61	0.68 0.93	0.5	1600	1.386	Si/SiO_2	Linear (cross)
[62]	460 650	---	---	---	---	1	Si/SiO_2	Linear (cross)
[63]	600 785 980	Above 60	---	0.58-0.85	NP1:circle NP2,3:rod	0.003-0.007	Au/Ti,glass	Insensitive
[64]	460 540 567 700	17.7 16 21.4 22.6	---	0.2	400	0.979 0.985 0.976 0.982	TiO_2/SiO_2,Ag	Insensitive

Note: “cross” refers to incident and diffracted beams which are mutually cross-polarized and “circle” refers to the circularly polarized incidence.

Table 2 Optical parameters of continuous achromatic metalenses

Reference	Wavelength (nm)	Efficiency (%)	FWHM (um)	Numerical aperture (NA)	Diameter (um)	Focal distance (mm)	Material	Polarization
[65]	1490-1550	50-60	---	0.28	500	0.85	Si/SiO_2,Al	Insensitive
		8.4		0.217		0.15		
[54]	1200-1680	12.44	1.5λ-2λ	0.268	55.55	0.1	Au/ SiO_2	Circle
		8.56		0.314		0.065		
	1300-1650		3-4	0.24	100	0.2		
[66]	1200-1400	Above 50	4.8-6.8	0.88		0.03	---	Insensitive
	1200-1650		2.5-3.2	0.13	200	0.8		
[67]	400-660	~40	2.5-3.2	0.106	---	0.235	GaN/Al_2O_3	Circle
		26.31		0.124				
[68]	400-667	22.74	3λ-5.8λ	0.165	41.86	0.163	Al/ SiO_2,Al	Circle
		15.03		0.198				
[69]	470-670	~20	---	0.2/0.02	6	0.063	TiO_2	Circle
[70]	460-700	35	---	0.075	1500	9.96	TiO_2	Insensitive
[71]	460-700	~92	---	0.2	26.4	0.067	TiO_2	Insensitive
[72]	3700-4500	~20.7	---	0.83	77.4	0.026	Si/CaF_2	Circle
[73]	$(3.75\text{-}10)*10^5$	Above 68	λ/2NA	0.385	10000	12	Based on Si	Circle

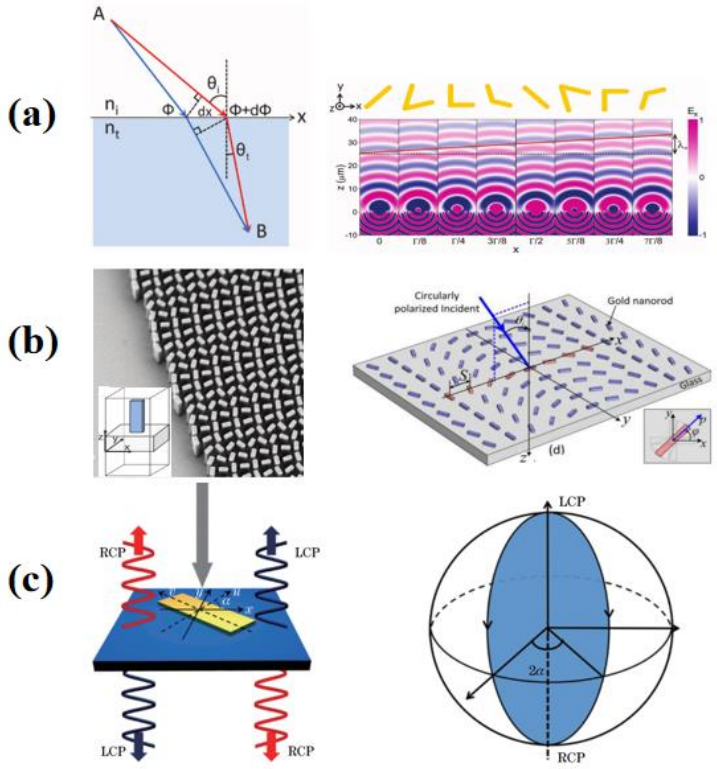

Fig. 1.a) Left: Schematics of generalized Snell's law of refraction; Right: V-shaped meta-atoms to abrupt phase in resonant phase metasurfaces[16], Reprinted with permission from Ref[16]. Copyright 2011, American Association for the Advancement of Science. b) Metasurface based on geometric phase modulation[8, 18], Reprinted with permission from Ref[8]. Copyright 2012, American Chemical Society. Reprinted with permission from Ref[18]. Copyright 2016, American Association for the Advancement of Science. c) Meta-atom illuminated by incident wave and scatters circular polarized waves and illustration of the principle of geometric phase by use of the Poincaré sphere[32]. Reprinted with permission from Ref[32].Copyright 201, CLP.

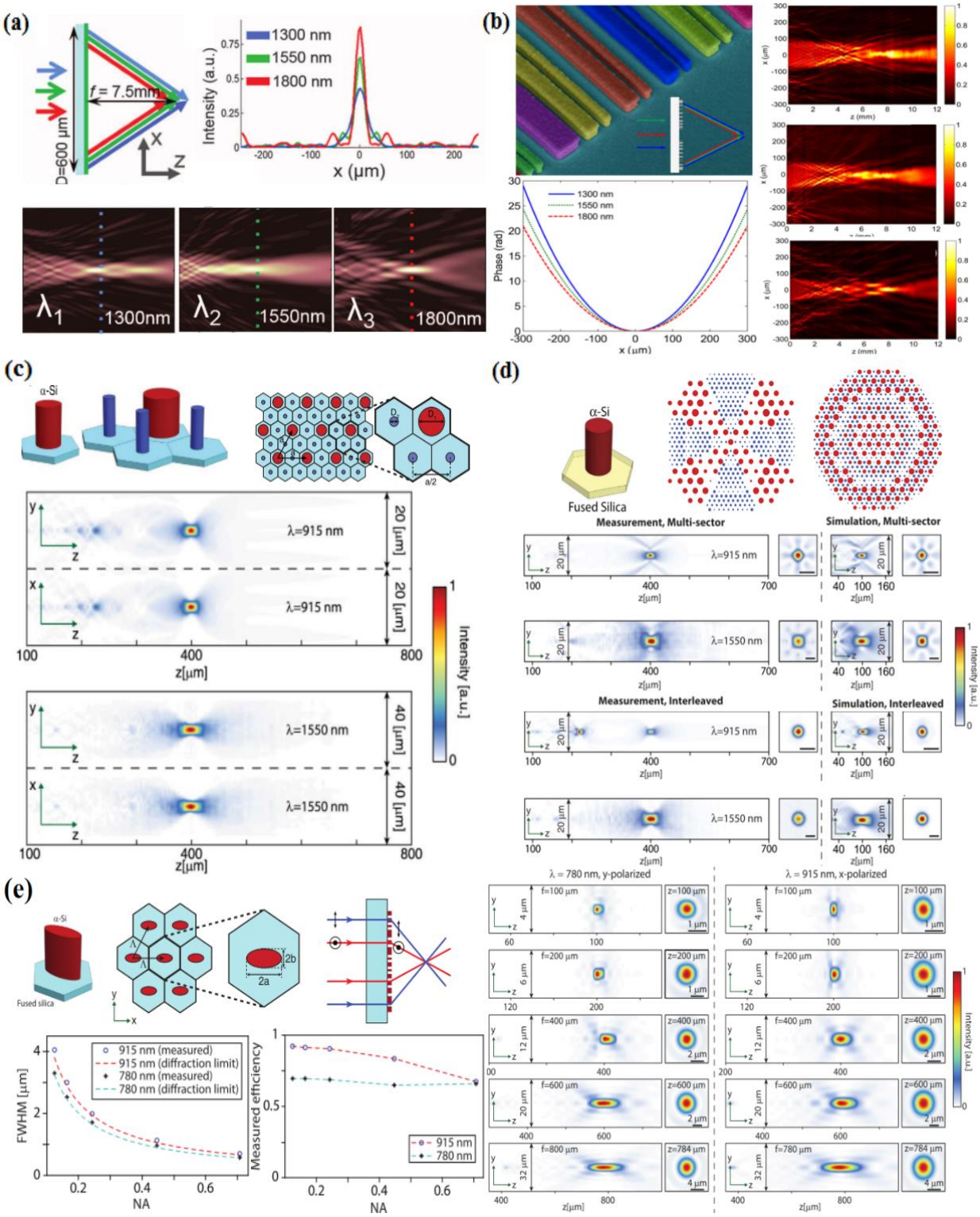

Fig. 2 Multiwavelength achromatic metalenses at infrared wavelengths range. a) Multiwavelength achromatic metalenses by dispersive phase compensation of 1300, 1550, and 1800 nm wavelengths[52]. Reprinted with permission from Ref[52]. Copyright 2015, American Association for the Advancement of Science. b) Metasurfaces consisting of coupled rectangular α -Si resonators at three wavelengths of 1300, 1550, and 1800 nm[55]. Reprinted with permission from Ref[55]. Copyright 2015, American Chemical Society. c) Multiwavelength polarization-insensitive metalenses with meta-molecules[56]. Reprinted with permission from Ref[56].

Copyright 2016, Optical Society of America. d) Polarization insensitive metalenses comprised of nanoposts in multisector lens (left panel) and interleaved lens (right panel)[57]. Reprinted from Ref [57] under the Creative Commons Attribution 4.0 International License (http://creativecommons.org/licenses/by/4.0/). e) Double-wavelength metalenses designed with birefringent elliptical meta-atom[58]. Reprinted with permission from Ref [16]. Copyright 2016, Optical Society of America.

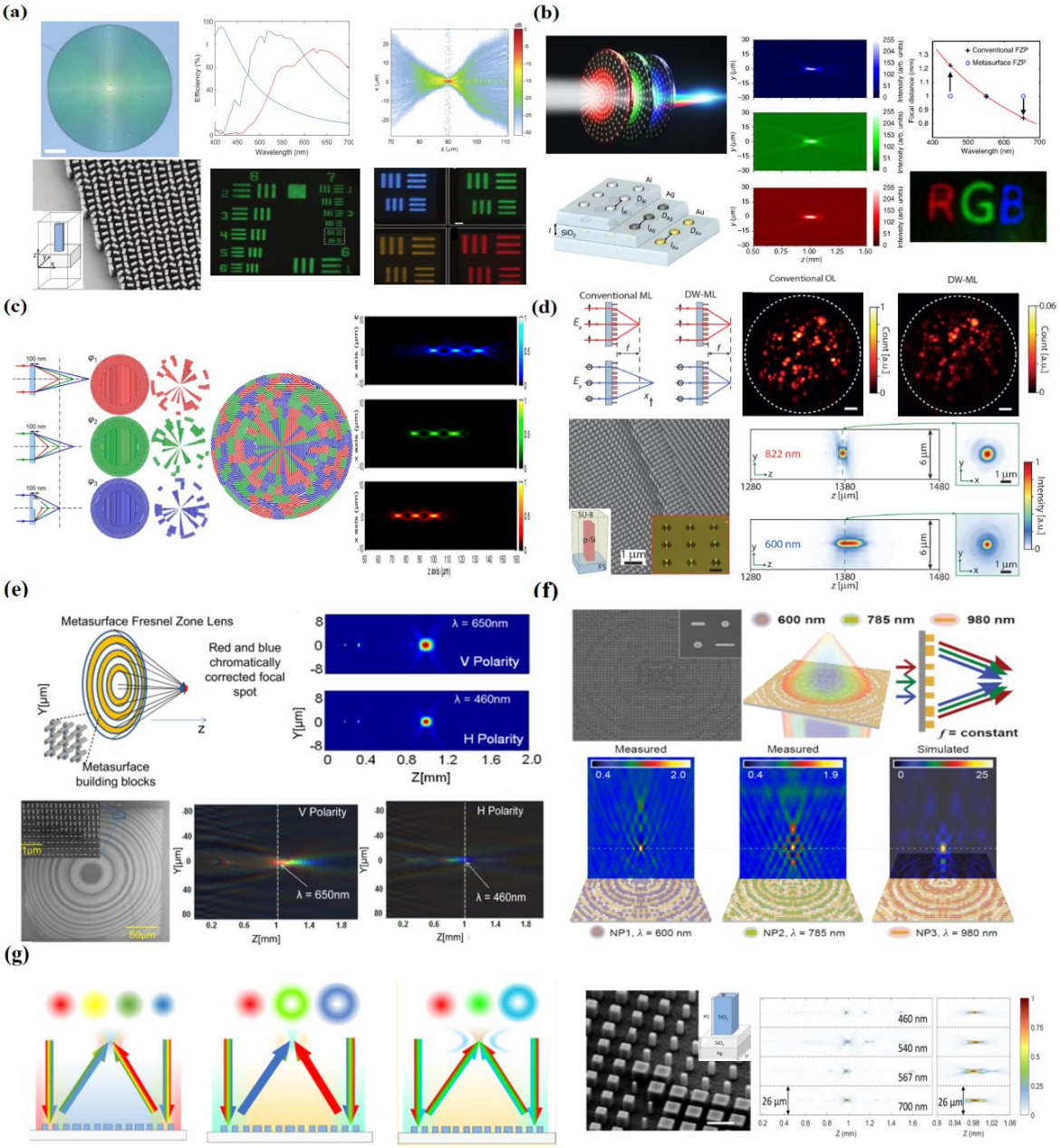

Fig. 3 Multiwavelength achromatic metasurfaces at visible wavelengths range. a) Visible-range metalens using TiO_2 composed of high-aspect-ratio nanopillars[18]. Reprinted with permission from Ref[18] Copyright 2016, American Association for the Advancement of Science. b) Vertical stacking metalens made of three different metallic nanodiscs showing the same focal distance at red, green, and blue light[59]. Reprinted from Ref [59] under the Creative Commons Attribution 4.0 International License (http://creativecommons.org/licenses/by/4.0/). c) Composite metalens consisting of three randomly segmented Si-based sublenses achieving light focusing at three

primary red, green, and blue wavelengths to the same focal length[60]. Reprinted with permission from Ref[60]Copyright 2016, American Chemical Society. d) Two-photon microscopy with a double-wavelength metalens based on polarization manipulating[61]. Reprinted with permission from Ref[61]Copyright 2018, American Chemical Society. e) Diffractive metasurface based FZP that corrects chromatic aberrations at pairs of wavelengths by polarization controlling[62]. Reprinted with permission from Ref[62]. Copyright 2015, Optical Society of America. f) Multiwavelength achromatic lenses based on subwavelength plasmonic nanoparticles using lattice evolution algorithm[63]. Reprinted with permission from Ref[63]. Copyright 2016, American Chemical Society. g) Multiwavelength achromatic metalens with achromatic focusing for blue, green, yellow, and red light and two wavelength-controlled beam generators[64]. Reprinted with permission from Ref[64]. Copyright 2018, American Chemical Society.

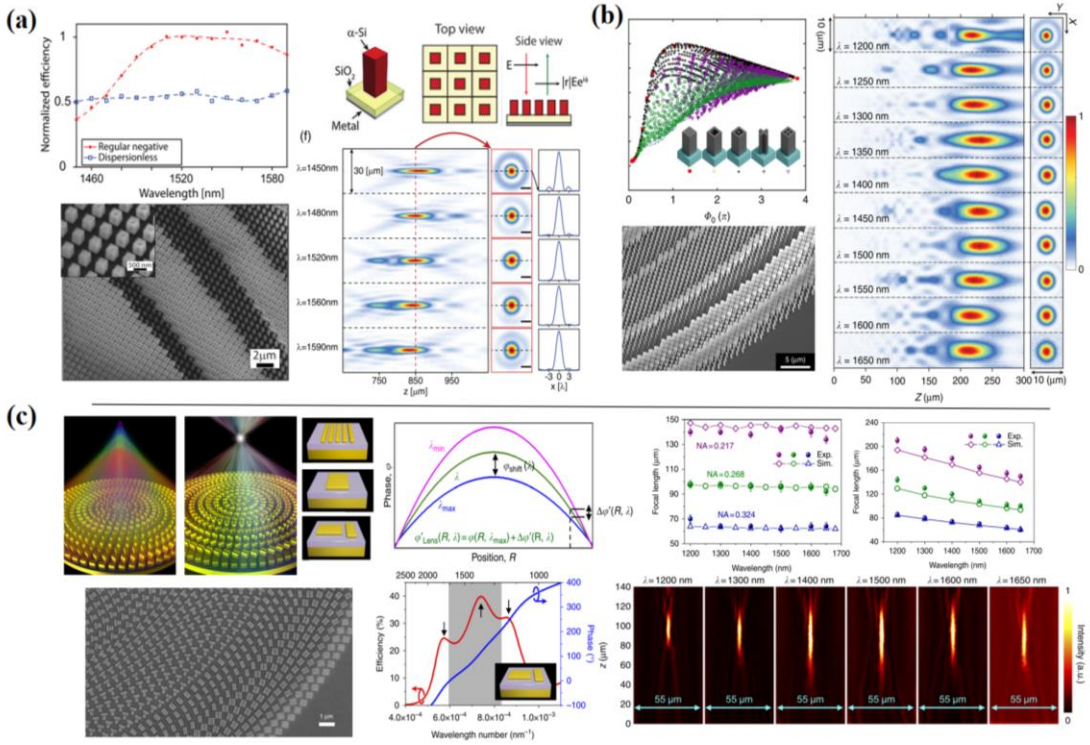

Fig. 4 Continuous achromatic metalenses at infrared wavelengths range. a) Dispersion-engineered metasurfaces with positive, zero, and hypernegative dispersions[65]. Reprinted with permission from Ref[65]. Copyright, 2017 Optical Society of America. b) Au integrated-resonant unit elements and new design principle and unvaried focal distance in a broad infrared bandwidth of 1200–1680 nm to realize broadband achromatic metalens[54]. Reprinted from Ref[54] under the Creative Commons Attribution 4.0 International License (http://creativecommons.org/licenses/by/4.0/). c) Broadband polarization-insensitive achromatic metalenses from 1200 to 1650 nm[66]. Reprinted from Ref[66] under the Creative Commons Attribution 4.0 International License (http://creativecommons.org/licenses/by/4.0/).

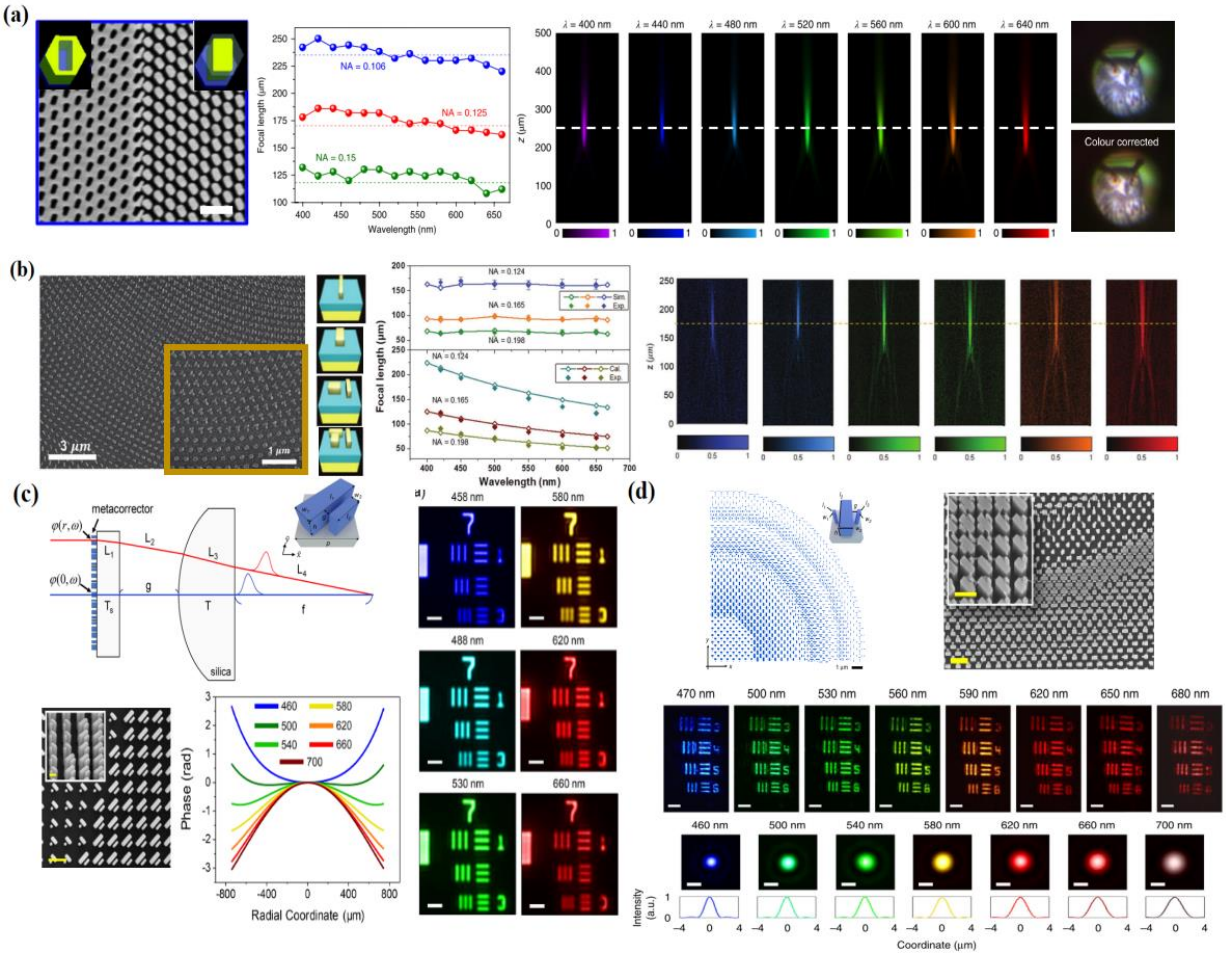

Fig. 5 Continuous achromatic metalenses at visible wavelengths range. a) Metalens made of GaN nanopillars and nanoholes to demonstrate a constant focal length from 400 to 660 nm[67]. Reprinted with permission from Ref[67]. Copyright 2018, Springer Nature. b) Visible Al-IRUs metalens achieving achromatic focusing from 400 to 667 nm[68]. Reprinted with permission from Ref[68]. Copyright 2018 WILEY‐VCH Verlag GmbH & Co. KGaA, Weinheim. c) Broadband achromatic metasurface-refractive device by combining metasurfaces and traditional refractive optical components[70]. Reprinted with permission from Ref[70]. Copyright 2018, American Chemical Society. d) Broadband achromatic polarization insensitive metalens over the visible range from 460 to 700 nm[71]. Reprinted from Ref[71] under the Creative Commons Attribution 4.0 International License (http://creativecommons.org/licenses/by/4.0/).

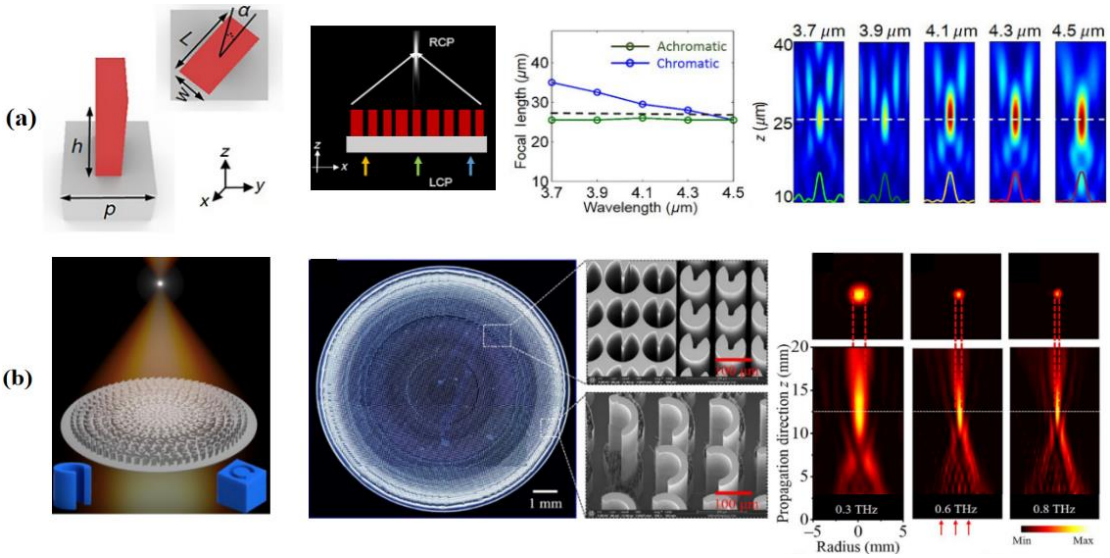

Fig. 6 Continuous achromatic metalenses at other range. a) Metalens made of Si nanobricks to realize an unchanged focal length in mid-infrared from 3.7 to 4.5 μm[72]. Reprinted with permission from Ref [72]. Copyright 2019, American Physical Society. b) Broadband achromatic metalens in terahertz regime from 0.3to 0.8 THz[73]. Reprinted with permission from Ref [73]. Copyright 2019, Science China Press.

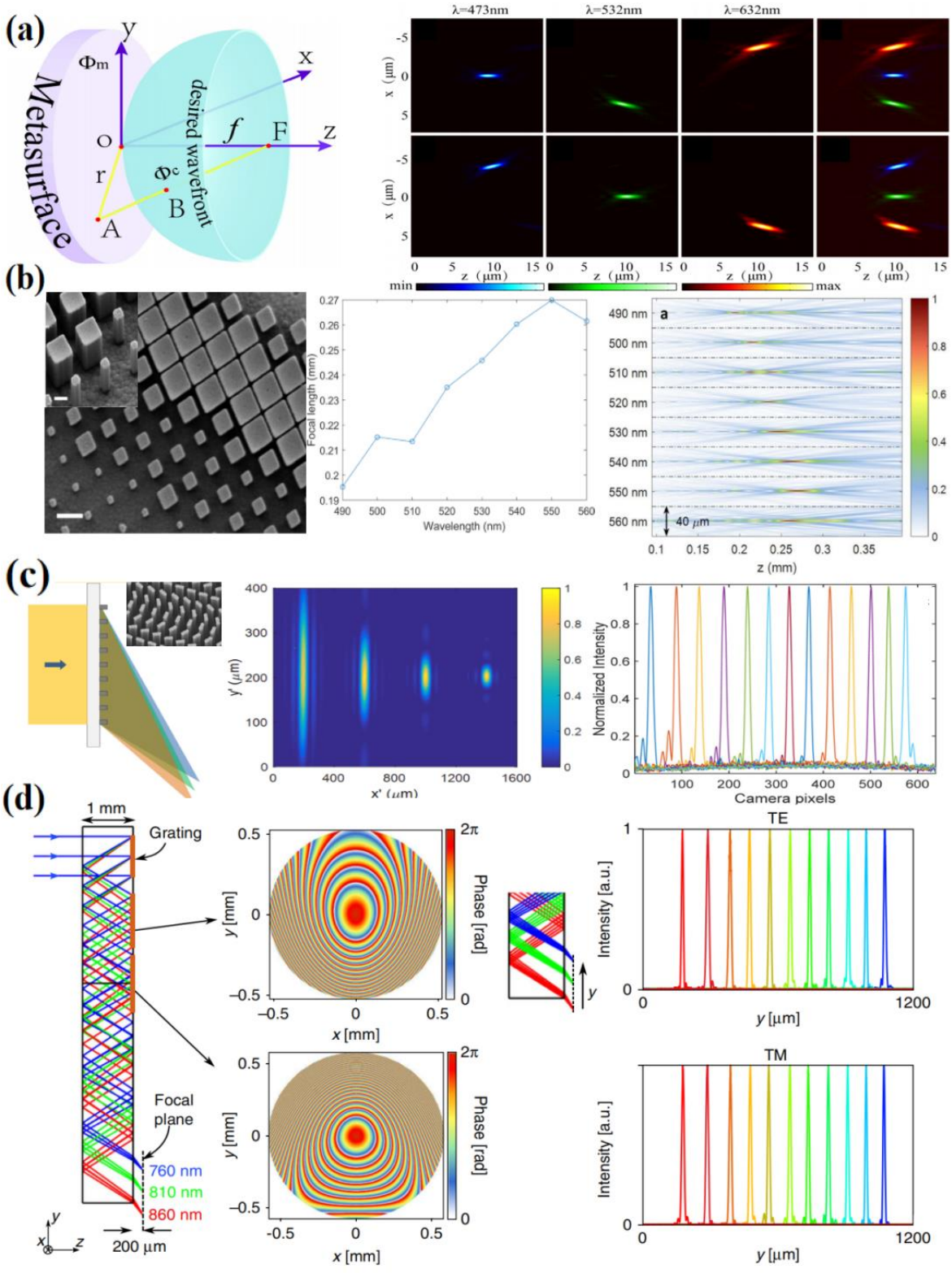

Fig. 7 Super chromatic metalenses. a) Multiplexing dielectric metalenses having realized arbitrary dispersion[74]. Reprinted with permission from Ref[74]. Copyright 2017, Optical Society of America. b) Metalenses with reverse chromatic dispersion design[75]. Reprinted with permission from Ref[75]. Copyright 2017, American Chemical Society. c) High spectral resolution realized by off-axis metalenses[76]. Reprinted with permission from Ref[76].Copyright 2016, American Chemical Society. d) Spectrometer consisting of three reflective silicon metasurfaces[77]. Reprinted from

Ref[77] under the Creative Commons Attribution 4.0 International License (http://creativecommons.org/licenses/by/4.0/).

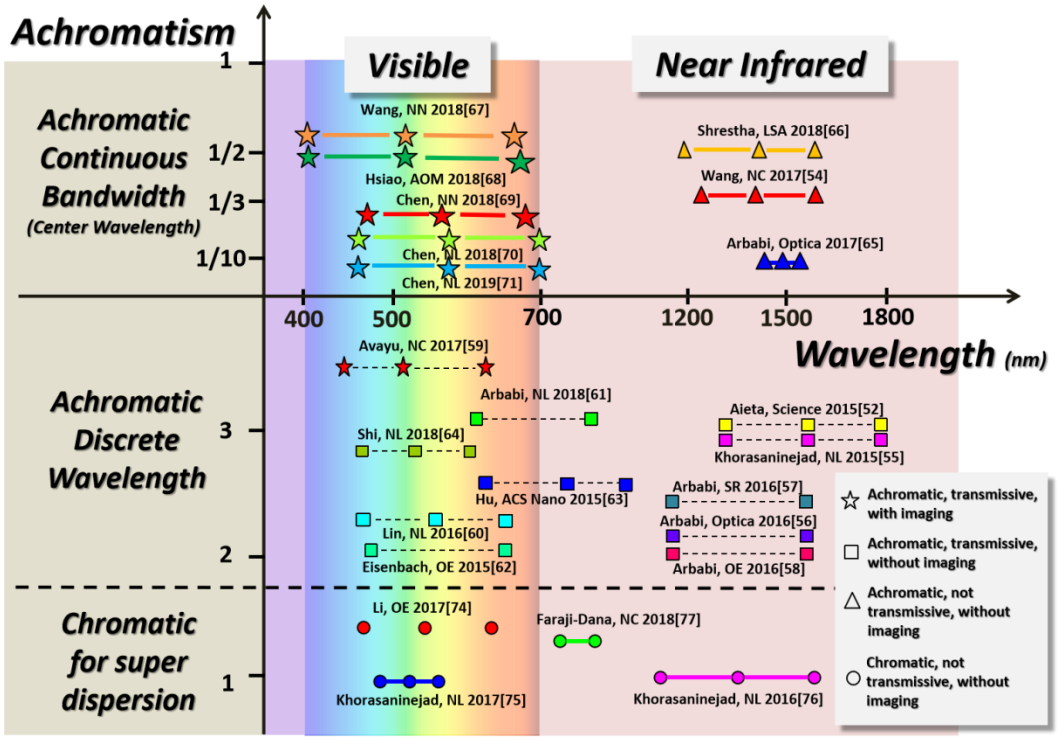

Fig. 8 State-of-the-art achromatic metalenses or super dispersion. The last name of the first author, the journal name, and the publication year are listed.

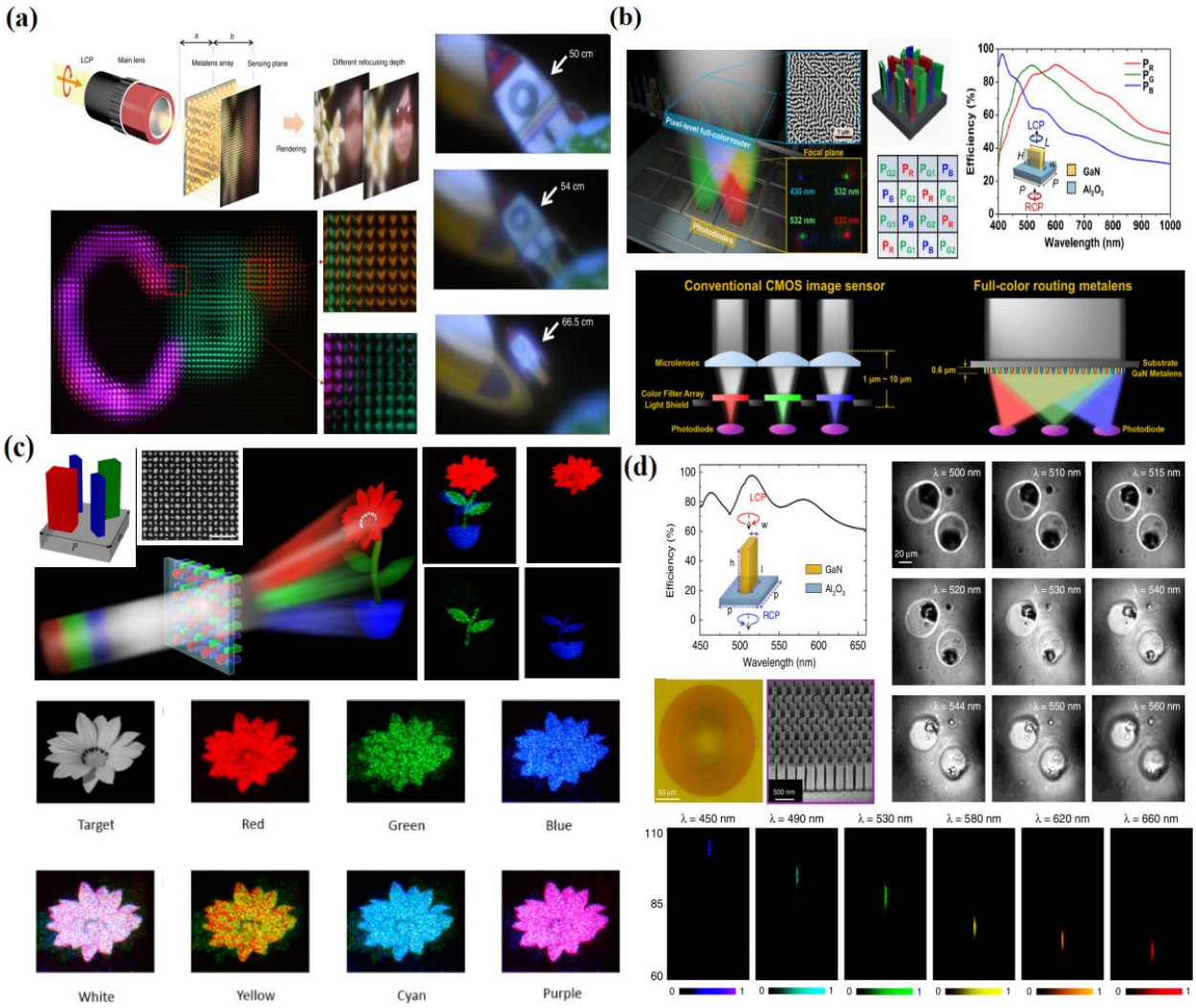

Fig. 9 Applications of achromatic and chromatic dispersion. a) Full-color light-field imaging captured by GaN-based achromatic metalens array[78]. Reprinted with permission from Ref[78]. Copyright 2018, Springer Nature. b) Multiplex metalens design for color routing in visible image[79]. Reprinted with permission from Ref[79]. Copyright 2017, American Chemical Society. c) Dielectric metasurfaces for multiwavelength achromatic and highly dispersive holograms[81]. Reprinted with permission from Ref[81]. Copyright 2016, American Chemical Society. d) Spectral tomographic imaging with aplanatic metalens[82]. Reprinted from Ref [82]under the Creative Commons Attribution 4.0 International License (http://creativecommons.org/licenses/by/4.0/).